Journal of Engineering Physics and Thermophysics, Vol. 75, No. 4, 2002

REVIEW

EFFECT OF SUPERDEEP PENETRATION. STATE OF THE ART AND PROSPECTS

O. V. Roman, S. K. Andilevko, S. S. Karpenko, G. S. Romanov, and V. A. Shilkin

UDC 534.2

The effect of superdeep penetration was revealed in the late 1970s and, before long, attracted the attention of researchers and was used as the subject of study for a number of original works. The experimental study of superdeep penetration was accompanied by the development of hypotheses concerning its physical explanation. The effort made by the researchers in different organizations to study the process made it possible to find a number of properties and characteristic features inherent in this phenomenon. The aim of the present work is to systematize and analyze the information accumulated at present, which must provide the basis for further investigations.

Introduction. Investigating the interaction of metal obstacles with dense powder fluxes accelerated by an explosion, Gorobtsov et al. [1, 2] have found that a part of the thrown powder material penetrates to depths larger than 10^2–10^4 gauges (a gauge corresponds to the characteristic dimension of a particle). The scale of the interaction was determined as follows [2–4]: discrete particles with a characteristic dimension of $d \sim 10^{-6}$–10^{-4} m penetrate into metals, and the part of the penetrating particles does not exceed 0.1% of the initial mass of the thrown powder. The result obtained was contradictory to the data accumulated in studying the results of the interaction of single strikers with solid obstacles (for example, [15–18]). It is easy to see that the interacting particles with any initial energy cannot penetrate to depths of the order of 10^2–10^4 gauges. Moreover, the existing theoretical models of penetration point to the impossibility of such a result, since to do this particles must have an energy content hundreds and thousands of times higher than that really attainable for the explosive accelerators used in [1–14]. Even if this energy is supplied to a particle, the depth of its penetration will remain comparatively small as usual because of the realization of a collision regime in which the interaction is accompanied by a thermal explosion [15, 19].

Properties of a Gas-Powder Flux Used to Obtain Superdeep Penetration. Data on only two schemes of acceleration of a powder, in which stable realization of the effect of superdeep penetration is possible, have been published at present. This phenomenon was found for the first time experimentally [1–3] as a result of the treatment of an obstacle with a gas-powder flux generated by an explosive accelerator whose schematic diagram is shown in Fig. 1 [3, 13, 20–23]. A numerical and experimental study of this scheme made it possible to determine the main parameters of the gas-powder flux produced by it [8, 23, 24].

It has reliably been established (both experimentally [23, 24] and theoretically [24, 25]) that this scheme produces a gas-powder flux which, similarly to a cumulative jet, consists of three main parts:

1. A high-velocity jet including up to 10–15% of the total mass of the powder and accelerated to 0.3–0.5D, where D is the detonation rate of the explosive used in the accelerator. In most cases, the velocity of the jet is 1–3 km/sec, but its density, as judged from the numerical results and experimental measurements, is relatively low. For the majority of powders (except high-density tungsten, lead, etc.) it does not exceed 1–1.5 g/cm^3.

2. The bulk of the flux (which takes the shape of a tunnel for a conical accelerator [24]) includes, as a rule, from 40 to 60% of the total mass of the thrown material. Its velocity does not exceed 0.1–0.3 D (less than 1 km/sec

A. V. Luikov Heat and Mass Transfer Institute, National Academy of Sciences of Belarus, Minsk, Belarus; email: rgs@itmo.by. Translated from Inzhenerno-Fizicheskii Zhurnal, Vol. 75, No. 4, pp. 187–199, July–August, 2002. Original article submitted October 18, 2001.

1062-0125/02/7504-0997$27.00

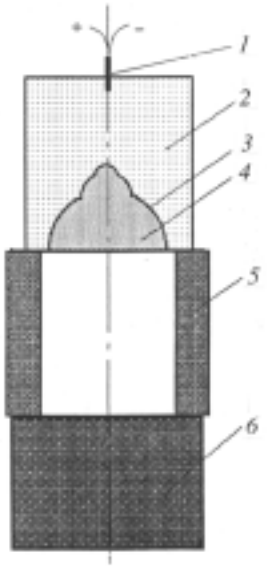

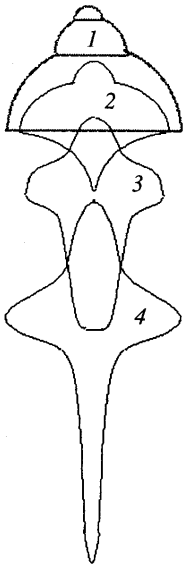

Fig. 1. Basic diagram of a cumulative explosive accelerator: 1) electric detonator; 2) explosive charge; 3) facing of the recess with a powder fill; 4) powder fill; 5) regulating support; 6) loaded specimen.

Fig. 2. Dynamics of the flow generated by a cumulative explosive accelerator: 1) initial position; 2–4) configuration of the flow with time.

in most cases). The density of this part of the flux is usually higher than the density of the high-velocity jet and is within 2–4 g/cm^3 for the majority of materials; its diameter is at least twice as large as the diameter of the high-velocity jet.

3. The pestle represents a low-velocity dense gas-powder flow with a mean velocity of 0.1 D or lower, which is 300–600 m/sec for the majority of real cases. Its density corresponds approximately to the density of the bulk of the material. The pestle can contain up to 40% of the thrown powder. In certain variants of the acceleration scheme, the pestle and the bulk of the material can merge together.

As follows from the foregoing, the gas-powder flow formed by an explosive accelerator which is shown schematically in Fig. 1 (hereinafter referred to as a cumulative accelerator) has a complex composition. The velocity and the density of the flux vary along the axis of symmetry within wide limits, which determines the nonmonotone character of loading. Its duration varies within 10^{-4}–10^{-3} sec under real-loading conditions depending on the parameters of the scheme and the chemical composition and the total amount of the powder and the explosive [25]. Figure 2 shows the dynamics of the flow formed by a cumulative accelerator; this dynamics has been constructed according to the results of the numerical experiments [25] verified by the real experimental data of [23]. The total amount of material accelerated by such an accelerator is ~70–300 g depending on the powder used. The total number of thrown discrete microparticles is ~10^{10}–10^{12}.

Figure 3 shows the basic diagram of acceleration of the powder used in [9–11] to stably obtain superdeep penetration. It differs significantly from the cumulative diagram (Fig. 1).

To produce a gas-powder particle flux Aleksentseva et al. [9–11] used, as a rule, a cylindrical RDX charge with a length-to-diameter ratio equal to 3, which provided the stationarity of the detonation process. The powder weights were 1 to 2 g [9], which caused the total number of discrete microparticles to decrease (to 10^8 to 10^9). In [9–11], an approximate calculation of the parameters of the accelerator used and the results of the experimental measurement of the rate of throwing of the powder are given. The calculation is based on the method of determining the parameters of one-dimensional throwing of bodies in separation of detonation products [26]. At a powder weight of 1 g and an explosive charge of ~63.6 g, the calculated time of acceleration was ~$4\cdot10^{-5}$ sec and the calculated rate was ~4–4.57 km/sec. The experimentally measured rate of throwing was much lower: ~1.8 and 2.2 km/sec [9] for weights of 1 and 2 g respectively. Such a marked difference between the calculated and experimental data is not accidental. It is predetermined by the use, in the method of [26], of the concept of throwing of a solid body differing significantly

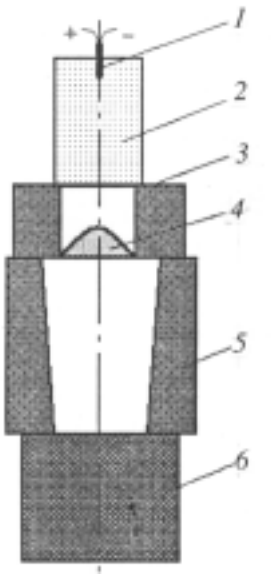

Fig. 3. Diagram of an explosive accelerator without cumulation: 1) electric detonator; 2) explosive charge; 3) metallic washer; 4) powder fill; 5) regulating support; 6) loaded specimen.

from that of a powder. Moreover, between the charge and the powder there is an air gap (Fig. 3) the existence of which is disregarded by the initial calculation procedure [26]. In this connection, for this type of accelerator the really attainable velocity of particles is ~2 km/sec. Judging from the oscillogram of the process of acceleration of particles presented in [9], the duration of loading exceeds 60 μsec (i.e., it is close to the values characteristic of the lower limit of the previous acceleration scheme). The pressure developed by the particle flux in the obstacle is ~1 GPa according to both the theoretical and experimental data [9, 11]. The velocity gradient along the axis of the particle flux is assumed to be much smaller than for the cumulative accelerator. The flux density, as judged from the velocity and the generated pressure, is close to that in the high-velocity part of the flux for the cumulative accelerator (~0.5–1.0 g/cm^3). Consequently, in contrast to the accelerator used in [1–8], the apparatus used in [9–11] generates only a part of the flow, which is separated as a high-velocity jet for the cumulative accelerator. The fact that superdeep penetration is recorded for both schemes allows the preliminary conclusion that it is precisely the high-velocity jet material that penetrates to superlarge depths; this part of the flux is self-sufficient. The question of whether the other two parts of the flow contribute to the process of superdeep penetration and of the value of this contribution remains unsolved, and it can be solved only on the basis of direct comparison of the results of penetration in the case of use of both acceleration schemes.

The general rule following from consideration of the operating conditions of the two throwing schemes using which one can stably obtain superdeep penetration can be formulated as follows: the phenomenon of superdeep penetration is observed in the case where the surface of a metal obstacle is treated with a high-velocity dense flux of a gas-powder mixture with a velocity of the front part of the flow of ~1–3 km/sec and a density higher than 0.5 g/cm^3.

Brief Description of the Basic Procedures of Experimental Investigation. The extraordinary nature of the phenomenon recorded in [1, 2] initially forced the researchers to focus their effort on a search for the proof of its existence. In this connection, superdeep penetration was recorded by highly diverse methods that can conventionally be subdivided into two large groups: recording of individual inclusions at large depths and quantitative estimation of the results of interaction. Moreover, procedures combining these possibilities have been developed in recent times.

The most vivid procedure of the first group is recording of inclusions by the devices of scanning electron microscopy. Metallographic sections of the obstacle material cut from it along the loading direction are used for observation. These sections are polished and pickled in an acid medium according to a special procedure [3, 13, 23], which is initially oriented to the primary removal of the obstacle regions subjected to the most intense plastic deformation. After the pickling, on the metallographic sections pretreated with a gas-powder flux there appear extended formations oriented mainly along the direction of treatment. Sometimes, these formations in the plane of the metallographic sec-

tion studied end with a cavity with the fragments of the striker (particle). Inclusions can be of different shapes, but most often the front part contains indications of smoothing. An x-ray microspectrum analysis carried out with the use of an attachment to the scanning microscope has revealed the high (up to 90%) content of the thrown material in the objects studied. This gives grounds to identify the inclusions as the fragments of microparticles and the above-mentioned extended formations as "channels" (tracks, trajectories) formed by particles in the obstacle material in the process of penetration, which closed ("collapsed") after the passage of the striker [3, 13, 23]. This is confirmed by the fact that the inclusions of the introduced (implanted) material carried away from the particle surface in the process of penetration are very often found in the "channels" after the pickling [3, 23] (when the procedure of pickling directed to the pickling of the strongly deformed material of the base is used, the introduced material sometimes remains undissolved). For certain types of powders (for example, Al_2O_3 [3, 5, 20]) one is able to observe fiber-like formations in the body of the "channel" [20, 23], which contain a large amount of the implantation material. The fact itself of detection of such inclusions and formations (especially in view of their not very large transverse dimensions (~1–15 μsec)) indicates that we are dealing not with single penetrating particles but with a certain part of the flux, even if not very large, but quite finite.

The results of the interaction of particles with an obstacle can also be demonstrated vividly with the use of the activation-analysis technique [27]. In this case the implanted material is selected such that the metallographic section studied becomes the source of specific radiation after the exposure to neutrons and γ radiation. Then the surface analyzed is brought into contact with a special detector film. The subsequent special treatment of the detector reveals the substance implanted and the character of its distribution over the plane of the metallographic section. This method can be used not only for direct detection of particles and their tracks, but also for quantitative analysis. Some results obtained by this method for an obstacle treated with a TiB_2 powder are presented in [23, 27]. They point to the existence of tracks of boron-containing inclusions, which pass continuously throughout the entire plane of the metallographic section (the section is cut in the direction of implantation of particles). By the density of these tracks one can estimate (both quantitatively and qualitatively) the efficiency of the superdeep penetration of TiB_2 into a steel obstacle.

The group of quantitative procedures for observation and investigation of superdeep penetration historically began with the chemical and electrochemical analysis [1, 3] of specimens for the presence of the implantation material in them. Such an analysis is based on the difference between the phases of the material in dissolution kinetics. Moreover, the methods of determining the content of the chemical element implanted from solutions by means of a layer-by-layer chemical analysis were being developed. Thus, the data providing the basis for investigations of superdeep penetration [1, 3, 9, 10, etc.] have been obtained. It should be noted that the procedure of electrochemical analysis can be used to determine the real size of the zones subjected to intense plastic deformation as a result of the passage of a particle through the material [13]. Unfortunately, data obtained by the method of chemical analysis are very difficult to analyze, because the amount of implanted material is relatively small.

For quantitative analysis of the results of penetration into metal specimens, the method involving determination of the visible porosity of a specimen before and after loading was also used. In this case, metallographic sections are cut in the direction perpendicular to implantation [3, 23]. They are ground and polished according to the standard procedure and then are pickled in an acid medium whose composition depends on the selection of the obstacle material and the powder thrown. A comparison of the visible porosity of the treated and initial materials revealed a certain dynamics of change of the porosity with depth of the obstacle, and this dynamics was different for different materials. However, it is still unknown what pores and what part of them can be associated with "channels" of penetrating microparticles, and what part is a consequence of the development of the structural inhomogeneity of the obstacle material in dynamic loading.

In recent times, attempts have been made to develop procedure for determining superdeep-penetration parameters on the basis of the results of treatment of special assembled specimens. This procedure has been mentioned for the first time in [13]. However, Shilkin positioned the objects (layers of a foil) in the front part of the assembled specimen and protected them from damage by a comparatively thin steel plate, which did not entirely exclude the possibility of the particles penetrating along the joints in the process of treatment with a flux of microstrikers. Subsequently, the procedure was improved substantially [25, 28, 29]. In this case, the working chamber is positioned in the back part of the specimen. In it, a stack composed of metallic-foil layers (the thickness of each layer is 10–30 μm)

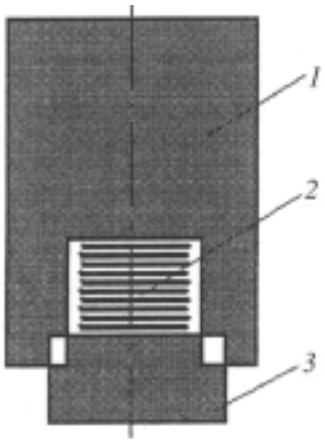

Fig. 4. Basic diagram of an assembled specimen: 1) loaded specimen with a cylindrical recess for the foil; 2) foil layers; 3) plug.

is placed (Fig. 4). Because of this, a complex obstacle with a great number of interfaces is along the path of penetrating particles entering the chamber after they have broken through the thickness of the front part of the assembled specimen, which provides their reliable deceleration [8, 13]. Initially, such an assembly was used to accumulate the implanted material, which was then subjected to a chemical analysis with the aim of determining the mass of the material penetrated to a depth equal to the thickness of the front part of the assembled specimen T [30]. However, for the majority of specimens studied the concentration of implanted material in the foil was low, which made the results obtained not very reliable, since they exceeded insignificantly the threshold of sensitivity of the methods of chemical analysis used. Because of this, in [25, 28, 29] the next step on the road to modernizing this experimental procedure has been taken. The size of the particles (~1–100 μm) allow them to be recorded on the foil by the devices of optical microscopy even with a 400–600× magnification, especially when the implanted material and the foil material are initially very contrasting in color. In this case, analyzing all the foil layers inserted into the chamber of the assembled specimen, one can determine the total number of penetrating particles and estimate (at least approximately) their size with the use of an optical microscope in reflected light. Analysis of the distribution of particles over the foil layers with allowance for the successive breaking of the latter makes it possible to construct the velocity distribution of the penetrating flux, determine the energy transferred by it, etc. [27]. Moreover, by decreasing or increasing the value of T for an assembled specimen treated according to the same scheme of penetration, one can determine the number of particles and the mass and energy of the penetrating flux at different depths. Knowing the initial conditions (the amount of implanted material delivered to the treated surface of the obstacle in the process of loading), it is easy, using the data on the change in the implantation parameters with depth, to construct the statistical picture of penetration and calculate the total amount of the implanted material [25, 28]. This method of analysis of superdeep penetration has received the name procedure of an assembled specimen.

Noteworthy is also the method of studying superdeep penetration by means of transmission electron microscopy [13, 23] (a 100B-computer microscope was used most often). In this case, blanks in the form of a foil 300–400 μm thick, cut by the electroerosion method from a specimen treated in the superdeep-penetration regime, were used for investigations. They were selected at a distance of 5–7 mm from the treated surface in the direction perpendicular to the implantation of the gas-powder flux. Then they were thinned by diamond pastes and electrochemical polishing. This method allows one to directly and carefully study the zone of the material located along the axis of penetration of the particle.

Quantitative information on the change in the characteristics of materials after superdeep penetration can be obtained by investigating their mechanical properties [13]. In this case, the commonly accepted procedures of measuring microhardness, hardness, bending strength, and impact strength are mainly used. We put emphasis just on the procedure that makes it possible to determine the ultimate breaking strength at different depths in steel specimens after the treatment by a particle flux. This is achieved by making a circumferential notch on round specimens [13].

There are also a large number of other procedures allowing one to evaluate the results of superdeep penetration, but the sphere of their application is much narrower than that of the procedures which have briefly been described above.

Results of Experimental Study of Superdeep Penetration. As has been noted above, even at the initial stages of study of superdeep penetration it was found [2, 3, 13, 14, 20, 31, 32] that the state of the obstacle material located along the trajectory of movement of microparticles differs significantly from the initial state. This difference is as follows.

1. It has been noted that when longitudinal (coincident with the direction of implantation) metallographic sections were pickled in acid media, the obstacle material along the trajectory of movement of particles is removed much more rapidly. The fact that extended structures pickled in such a manner are actually located along the axes of the trajectories of the penetrating particles is confirmed by two facts: a) every so often such formations end with a pickled cavity containing the remainder of a microparticle (the shape of the cavity as a whole corresponds to the shape of the remainder, and the fact that this is precisely the remainder of the implanted particle is confirmed by a chemical test); b) chemical samples taken from these zones contain a marked part of the implantation material and, in certain cases, such zones have the appearance of fibers or filaments remaining in the "channel" cavity after the pickling [20, 23]. The high rate of removal of the material in these zones is explained by the very high degree of imperfection of the structure caused by local plastic deformations arising as a result of the interaction of the moving particle with the obstacle.

2. Investigations of transverse (perpendicular to the direction of implantation) metallographic sections by the methods of diffraction electron microscopy have shown [23, 33, 34] that the obstacle material directly adjacent to the axis of the trajectory of movement of particles in the narrow zone $\leq d$ loses the long-range order characteristic of metal structures. The estimations made in [35] suggest that this is a result of rapid heating (crowning the plastic interaction of the particle with the obstacle) and of the very rapid subsequent cooling (cooling begins immediately after the particle passes through the cross section considered). The state of the material in this zone is defined as x-ray amorphous. A region of diameter 2–3d filled with a substance whose structure can be defined as highly defective with a high density of dislocations is directly adjacent to the zone of the x-ray amorphous material. With distance from this zone, the degree of imperfection of the structure rapidly decreases. In the process of pickling, the material from the zones of x-ray amorphization and high imperfection is removed first, which made it possible to observe particle tracks in the matrix material.

3. It is noted that when a striker is found at the end of the track, the shapes of the particle and of the cavity as a whole correspond to each other [5, 8, 34]; the structure of the obstacle material near the stuck particle is similar to that observed in investigating transverse metallographic sections. The shape of the found fragments of microparticles substantially depends on their nature. For refractory and brittle compositions (TiB_2, TiCN, etc.) the fragments of strikers have a chippy shape, although on their front parts there are roundings arising as a result of the interaction with the obstacle material. The fragments of metal powders which are found in pickled cavities adjacent to the end of the tracks are usually drop-like in shape. This points to an intense removal of the implanted material from the particle surface in the process of penetration (most probably, it is removed in the form of a melt and is mixed with the base).

Channel zones have been found in all the metal materials studied [3, 8, 13, 23] (steel, Cu, Ti, Al). In steel, "channels" could run along both the ferrite and perlite (or mixed) structural elements. The investigations show that the "channels" formed cannot be considered to be strictly rectilinear. They can bend [3, 8, 23], retaining the predominant orientation in the direction of treatment. When particles meet foreign inclusions, they can both break through them or deviate from the initial direction of motion [23, 31, 32]. At the same time, it is beyond reason to advocate that the boundaries of the grains in any way influence the "channels." In the majority of observations, tracks crossed the boundaries of the grains without any visible changes in the direction or the structure [8, 13, 14, 20, 23, 31, 32].

A study of the behavior of particles near the interfaces of different materials made it possible to find one more subtlety that has not yet received an exhaustive explanation [36]. Thus, tracks formed by certain implantation materials in obstacles begin to turn as an interface of the steel–titanium or steel–copper type is approached (the free surface of the first material, steel in this concrete case, was subjected to loading) well before they intersect the separation surface, reaching the trajectory tangential to this interface. In the case of loading on the back side (on the side of the free surface of copper and titanium), such tracks were not observed. It should be noted once again that the tra-

jectory begins to turn well before the track contacts the interface and the distance between the particle and the interface is ~4–6*d* at that instant. The NbB_2 powder (fraction 1–10 μm) is used as the thrown material, and the metal layers are united into a single bimetallic target by the method of explosion welding. The chemical analysis of the bimetallic obstacle, along with the metallographic analysis, showed the presence of boron in both parts of an obstacle of the Fe–Fe type, only in the iron layer of obstacles of the Fe–Ti type, in iron, and in the 40-micron Cu layer adjacent to the interface in an obstacle of the Fe–Cu type (an analysis for the presence of niobium was not made unfortunately). This phenomenon and the fact that the chemical analysis did not reveal the presence of boron when attempts were made to implant it, as part of different compounds, into titanium and copper (whereas the penetration of other boron-free powders into these metals was reliably detected) enabled one to suggest that there exists a certain chemical selectivity of superdeep penetration [23, 36]. Unfortunately, the latter has not been checked for other powders, which makes it impossible either to confirm or to reject such a conclusion. However, bimetallic obstacles were investigated for other purposes and by other methods, which will be mentioned below.

Investigations of a change in the visible porosity of the obstacle material in specimens loaded according to the procedure of superdeep penetration have enabled Usherenko [3, 23] to infer that mixture compounds which consist of powders different in chemical composition (for example, 50% SiC + 50% Ni) reveal higher efficiency in penetration than powders formed on the basis of a single compound or chemical element. It was established that a certain relationship between the size of the initial thrown particles and the size of pores visible on transverse metallographic sections and their amount exists [3, 37]. Unfortunately, work on classification and identification of the detected pores remains to be finished, which makes it impossible to properly use the accumulated experimental material.

The use of a chemical analysis for recording of the powder implanted into the obstacle material made it possible to accumulate quantitative information on the process of superdeep penetration. The most substantial difficulty associated with the use of chemical analysis is that the total amount of implanted material is small (no larger than 0.1% by weight [38]), whereas the initial metal can also contain this material in the form of impurities. Because of this, the data of chemical analysis strongly depend on frequent occasions on the method and site of obtaining them. It is very difficult to determine exact and stable values of the concentration of the implanted element; this being so, only the general regularities of their change were taken into consideration. Nonetheless, it was established that:

1. In the case of penetration of powder materials whose solid phase is formed by two elements or more (for example, powders of TiB_2, TiCN, SiC, etc.) the concentration of different elements entering into the composition of the solid phase can change in different ways in the depth of the obstacle. Their local extrema can differ from each other in this case [23, 39]. This points to the complex character of the removal of the material from the surface of penetrating particles, where, because of the high temperatures, the compounds can dissociate and different elements can lose their mass in different ways.

2. The mass of the particle can change (decrease, as a rule) continuously and discretely when a certain, frequently large part of the striker is removed [38, 40]. The possible discreteness of the removal of the mass of a particle can have a marked influence on its motion due to the rapid (practically instantaneous) change in its size, mass, and symmetry, which in turn causes a jump-like change in the parameters of motion of the striker (for example, the direction of movement).

3. Materials having different physicomechanical properties penetrate into an obstacle in different ways [9, 10, 23]. Thus, according to the data of [9], the maximum concentration of titanium implanted into copper amounts to 0.5% (the average concentration is ~0.1%) while the maximum concentration of chromium amounts to 0.1% (the average concentration is ~0.006%). For the tungsten powder (in the case of its penetration into titanium) the maximum concentration amounted to ~0.05% while the average concentration amounted to about 0.02%. In the case of implantation of chromium into aluminum, the maximum concentration reaches ~0.02%, while the average concentration reaches ~0.014%. In this case, we are dealing, of coarse, with the deep-lying layers of the treated obstacles, since near the loaded surface the concentration is much higher and can reach several percent.

4. The concentration distribution of the implanted material in the depth of an obstacle is nonlinear and nonmonotone in character [3, 8–11, 13, 41]. In [9, 10], it is inferred that the concentration changes quasiperiodically in the depth of the obstacle. Moreover, there are scattered data (for example, [9]) which also point to the fact that the concentration changes quasiperiodically in the centerline (perpendicular to the direction of implantation) plane of a specimen. It should be noted that although the case in point is the quasiperiodicity of the change in the concentration

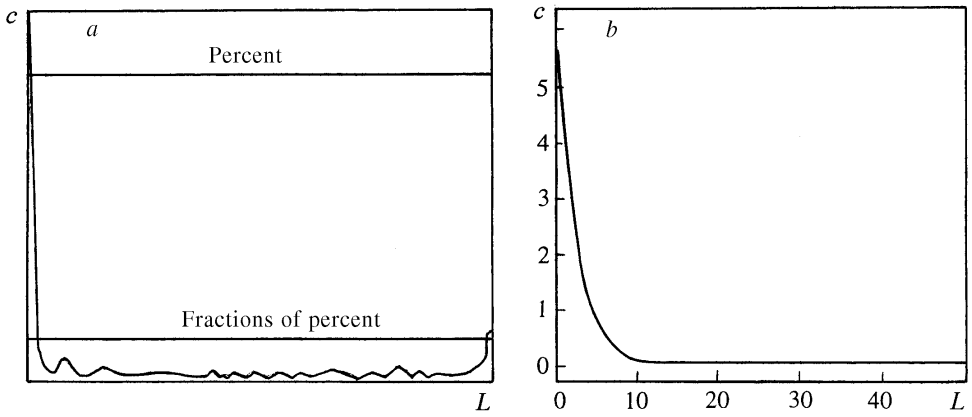

Fig. 5. Dependence of the concentration of the implanted material on the depth, obtained experimentally as a result of the chemical analysis (a) and calculated from the experimental data with the use of the procedure of an assembled specimen (b). *c*, %; *L*, m.

with depth, the general (global) character of its change can be considered as monotonically decreasing when the quasiperiodicity of the change in the concentration manifests itself as a number of local maxima and minima. The general picture can be presented by the basic dependence of Fig. 5a or by the curve constructed on the basis of the experimental data on the penetration of tungsten into steel [42] (Fig. 5b) (*c* is the concentration of the implanted material by weight in percent). A characteristic feature is a sharp decrease in the concentration near the loaded surface (from several percent on the surface to tenths of a percent at a depth of 1–2 mm). Then the concentration varies between ~0.01–0.2% and increases by 20–40% as the free (unloaded) surface of the obstacle is approached (the latter is a very characteristic feature of superdeep penetration). Judging from the data of [9], the concentration in the centerline plane of a specimen varies within a much narrower range. While on the subject of the periodicity (or quasiperiodicity) of the change in the implanted-material concentration with depth, Usherenko et al. [3, 9, 10, 13, 41, 42] do not indicate the duration of this period. It is believed that in this case it is necessary to perform much finer experiments with a shortened "step" of depth measurements. It should be emphasized that since superdeep penetration is characterized by a large number of interacting objects (the initial number of particles is $\sim 10^8$–10^{12} depending on the loading scheme and their size), the process of penetration is inevitably static in character. This means that the more statistically justified the experimental data, the greater the confidence in them. A much more statistically reliable set of experimental data is required to elucidate conclusively the question of the periodicity of superdeep penetration.

The question of the characteristic limits of the change in the concentration of the material implanted into an obstacle as a result of the process of superdeep penetration was the subject of investigation and discussion throughout the period of investigation of the effect. Clearly, the concentration distribution of the implanted material in the depth of the obstacle characterizes the efficiency of the loading scheme used not in full measure. It is no less important to know which part of the thrown material penetrates into the obstacle to so large distances. Starting from the general considerations, the authors [43] estimate this value at hundredths of a percent of the initial amount of the thrown material. The above-mentioned procedure of an assembled specimen makes it possible to answer this and a number of other questions with a sufficient degree of accuracy [25, 28, 29]. In [25, 29], the number of particles on the foil layers placed in assembled specimens with a different front thickness which are treated according to the standard procedure [23] of superdeep penetration is estimated with the use of the cumulative scheme. The number and size of particles that passed throughout the entire front part of the assembled specimen are measured. Normalizing these data to the total amount of the material used for acceleration and throwing, the authors [25, 29] obtain information on the total number of implanted particles and its change in the depth of the obstacle. This dependence allows one to construct a curve of change of the concentration of the implanted material in the depth of the obstacle (Fig. 5b). Calculating the area under the curve in Fig. 5b, one determines the total content of the implanted material. In a steel target treated with a copper powder of fraction 50–63 μm [25] this value was 0.0007961 kg, or 0.39% of the entire material thrown by the accelerator. However, if one fails to take into account the particles penetrating into the obstacle to a depth of

$\leq 10d$, which is quite attainable even beyond the superdeep-penetration limits, the effective mass of the material penetrated in the superdeep-penetration regime will be much smaller and be equal to $\sim 8.535 \cdot 10^{-5}$ kg, i.e., about 0.04% of the initial amount of the material, which is quite in agreement with the conclusions of [43]. Determination of the velocity of the particles recorded on different foils made it possible to construct the curve of their velocity distribution. The mean velocity of movement of the particles was ~400 m/sec. This value should be considered as preliminary, since it depends on the minimum rate of breaking through the foil, which can vary within very wide limits depending on what data are used to determine it.

A specific behavior of penetrating particles is observed at the interfaces of metals with a different density. The general study of bimetallic obstacles of the Fe–Ti, Fe–Cu, Ti–Fe, Cu–Fe, Ti–Cu, and Cu–Ti type and of multilayered (sandwich) structures of these materials by the method of sampling for chemical analysis of the presence of the implanted material has shown that in the regions adjacent to the corresponding interfaces the concentration of the implanted material (cobalt and tungsten) is somewhat increased. However, in distinction to boron in [36], this increase is recorded in all the layers studied.

Modeling of superdeep penetration in the context of thermoplastic interaction of particles with the obstacle material [44–46] makes it possible to integrate the motion of a particle in the layer where we have a jump-like change in the density of the target material [47]. In this case, it has been established that at an interface of the less dense–more dense material type the velocity of the particles decreases rapidly and for combinations of the Al–Pb type we can have a complete termination of penetration of particles ("suppression" of superdeep penetration) in some regimes of loading. The experimental check of this conclusion with the use of both the chemical analysis and the procedure of an assembled specimen [47] fully confirmed these conclusions. It has been noted that the efficiency of penetration through metal obstacles of the Ti–Fe, Al–Fe, Fe–Pb, and Ti–Pb type decreases generally and penetration through an interface of the Al–Pb type is "suppressed" (absent) completely, in practice (as in the previous cases, the loading was made on the source side of the free surface of the material indicated first in the notation of the type of interface). However, in the case of combination of layers of different materials, the density change is not quite jump-like. On each side of the imaginary interface there is a layer, if even very narrow, where the density changes relatively smoothly from the initial value for one metal to the initial density for the other. A minimum deviation of the trajectory of a particle from the normal to the interface can cause the striker to turn and slow down along the curvilinear trajectory, which is even more probable in view of the fact that the shape of the powder particles used in practice is far from being ideal. Conceivably, it is because of this fact that in the experiments of [47] the efficiency of the scheme generally decreased for any bimetallic targets used (as compared to monometallic targets), although in the method of construction of an interface of the more dense–less dense material type such a decrease was much less marked.

In a number of experiments on determining the dependence of the visible porosity on the fractional composition of the thrown materials [3, 23], it has been noted that the number of pores decreases markedly when an obstacle is loaded by a flux of particles with a size of >100 μm, from which it was inferred that there is a limiting size of particles that can penetrate into obstacles by the superdeep-penetration mechanism. Formally this size was estimated at 10^{-4} m, but no special investigations on this problem were conducted. Pointing to the possibility of existence of this limiting size, we note that in the future it is necessary to determine its value more exactly and analyze its dependence on the character of loading and the geometric dimensions of the accelerator.

A number of investigations [11, 48] were devoted to studying the density of the treated obstacles after the superdeep penetration. It has been established that the average density of steel obstacles somewhat increases after their treatment with denser materials (powders of tungsten and cobalt). For less dense powders (Al_2O_3, TiCN, etc.) the reverse tendency has been noted. Treatment of a steel obstacle with iron powders of various fractions had a much smaller effect on the density change. The attempts to obtain the same dependence for aluminum and titanium have not met with success. Density changes were also noted there, but they were much less organized in character [11].

Among the most complex problems of study of superdeep penetration are problems of repeated treatment of an obstacle with a gas-powder flux. This is explained by the fact that in the case where chemical analysis is used as the recording method, the same specimen cannot be subjected to repeated loading, since it must be cut after a certain number of loading cycles to determine the concentration of the implanted material. Nonertheless, in the case where cutting and chemical analysis of steel obstacles were made only after the attainment of the required multiplicity of

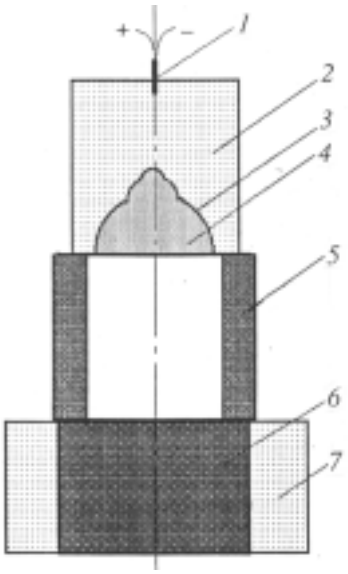

Fig. 6. Scheme of acceleration with additional pulse loading: 1) electric detonation; 2) explosive charge; 3) facing of the recess with a powder fill; 4) powder fill; 5) regulating support; 6) loaded specimen; 7) additional explosive charge synchronized with the accelerator.

loading, it was possible to elucidate that there is no marked difference between the first and the second cycles of loading, but the third and the fourth cycles differ markedly [42]. In particularly, in the third cycle of loading the concentration of the implanted material markedly increased, while in the fourth cycle the concentration somewhat decreased. However, the conclusion (drawn in [23]) that the material is removed in the fourth cycle seems to be somewhat premature, since different specimens were subjected to loading. Nonertheless, the fact that the fourth cycle of loading fundamentally differs radically from the third one is supported by a series of experiments carried out according to the procedure of an assembled specimen, where the foil layers were removed for analysis after each cycle and were replaced by new ones [49] for the next cycle of loading. The numbers of particles recorded on the foil in the first three cycles of loading were comparable (four assembled specimens with a different thickness of the front part were subjected to loading). The fourth cycle was characterized by the double and even triple increase in the number of detected particles, which, undoubtedly, point to the fact that the penetration in this case differs qualitatively from the penetration in the previous cases. It should be noted that in this case, all four cycles of loading were carried out on the same specimens, since there was no need to cut them.

The obvious pulsed nature of the process of superdeep penetration leads to the question: How will the results of superdeep penetration change if one more pulsed source (besides the accelerator of powder particles) of energy delivered directly to the obstacle is put into operation [8, 23, 50, 51]? As such a source, we used an explosive charge positioned along the side surface of the obstacle and synchronized with the accelerator (Fig. 6). The results of some experiments have shown that the concentration of the material implanted into the obstacle in the superdeep penetration regime was markedly increased, although the attempts to obtain fully stable and recurring results have not met with success in this case.

The most substantial and systematized investigations of the influence of superdeep penetration on the mechanical properties of steels have been carried out in [13]. A powder flux was formed by a cumulative accelerator. It has been established that superdeep penetration leads to the improvement in the hardness and the ultimate breaking strength near the surface on the source side of treatment with the powder flux. This effect is most pronounced on low-carbon steels (for example, for 10 steel treatment with a TiB_2 powder flux increases the ultimate breaking strength by 41% at a depth of 7 mm and by 19% at a depth of 11 mm). A change in the chemical composition of the powder leaves the tendency unchanged — the strength and the hardness reach maximum values near the surface treated with particles, then they sharply decrease to the initial values at depths of ~18–25 mm. The character of the change in the parameters with depth is analogous to that in the case of action of shock waves. Treatment of 10 steel with a high-

velocity powder flux leads to the anisotropy of the strength — the ultimate breaking strength increases in the direction coincident with the direction of implantation of powder particles and remains unchanged in the transverse direction. All the materials (carbon steels) investigated in [13] are as follows in order of decrease of their capacity for strengthening: 10 steel, 20 steel, U10A steel, 45 steel, and U7A steel. It is of interest to track the combined action of superdeep penetration and heat treatment. It has been established that lengthy annealing eliminates the entire strengthening caused by superdeep penetration. This indirectly confirms the fact that a small amount of the material is implanted into the obstacle. At the same time, superdeep penetration decelerates the processes of softening in tempering the hardened steel, and the higher the tempering temperature, the more pronounced this tendency. Elements implanted into the steel in the superdeep-penetration regime are localized in small volumes of the material adjacent to the channels and have a strengthening effect on them. Steels with a high content of alloying elements (for example, high-speed steels) act differently. Their strengthening in the course of superdeep penetration is small, but it propagates to comparatively large (30–40 mm) depths. The greatest gain in properties is attained by combination of the optimum regimes of superdeep penetration and heat treatment; powder particles penetrating into the ferrite component of steel not only interact crystallochemically with the matrix, but also form the zones of an intensely plastically deformed material. In these zones, in the case of subsequent heating for heat treatment, the alloying elements diffuse with high velocities from the surrounding layers of the material, which results in the formation, in the structure, of carbide chains extended in the direction of implantation of powder particles. Such materials possess good mechanical properties.

Thus, the experimental study of the process of superdeep penetration made it possible to determine a number of features inherent in it and to develop and use in practice procedures contributing to statistically competent study, description, and classification of the phenomenon and its use for practical purposes.

Basic Hypotheses Aimed at Explaining and Modeling Superdeep Penetration. The complex conditions of realization and observation of the effect stimulated the effort that went into adequate theoretical interpretation of it. This explains the large number of original assumptions made in modeling and the complexity of the experimental check of the conclusions drawn by the authors of different models. All the models known to the authors of this work can conventionally be subdivided into three groups depending on what character of interaction of the particle–obstacle system was used as the basis for modeling: 1) brittle models constructed on the assumption of specific conditions of cracking in the case of superdeep penetration; 2) plastic models based on the development of the notions of softening (complete or partial) of the material in the region of interaction and the collective character of the process; 3) shock-wave models explaining the existence of superdeep penetration by the specific interaction of shock waves with the obstacle or with the implanted particles.

1) *Brittle models.* The first assumptions on the development of specific types of cracks leading to superdeep penetration have been formulated and published simultaneously in [6, 7]. The notion of a small expenditure energy required for the development of a crack once it has been formed was used for modeling of superdeep penetration. It was assumed [6] that the brittleness of a metal specimen must correspond to the brittleness of glass. This was explained in [7] by the plasticity delay. It was also assumed that the crack behind the particle must close (collapse); the expenditure of energy on heating and the afterflow (creep) were ignored. In [52, 53], an attempt was made to estimate the afterflow made by the collapsing crack. However, since the study of metallographic sections (the data appeared much later than [6, 7]) perpendicular to the direction of implantation did not give any grounds to assume that a crack develops in these zones, there appeared the idea (purely qualitative) of quite a specific formation, i.e., a "circular crack" [54]. The uncertainty of the properties of this structure and of the characteristics of its development and motion kept the author of the model from making any substantial progress toward studying the actual properties of the superdeep-penetration effect and in its modeling. In our opinion, the main disadvantage of the modeling of superdeep penetration with the use of specific assumptions of the special properties of brittle interaction is their total indifferentness to experimental data.

2) *Plastic models.* The necessary condition of existence of superdeep penetration within the framework of such models even at the earliest stages of their development [4, 8, 50, 51] was the assumption of the general partial disordering of the obstacle material in the period of its loading by a particle flux. In local regions with an impurity or defect structure, such disordering could be total. The action of the powder-particle flux was considered as a repeated loading of the obstacle by individual elements of the flux structure and by the layers of particles colliding with the obstacle. Such an action "rocks" the crystalline lattice and enables the structure to store and redistribute the flux

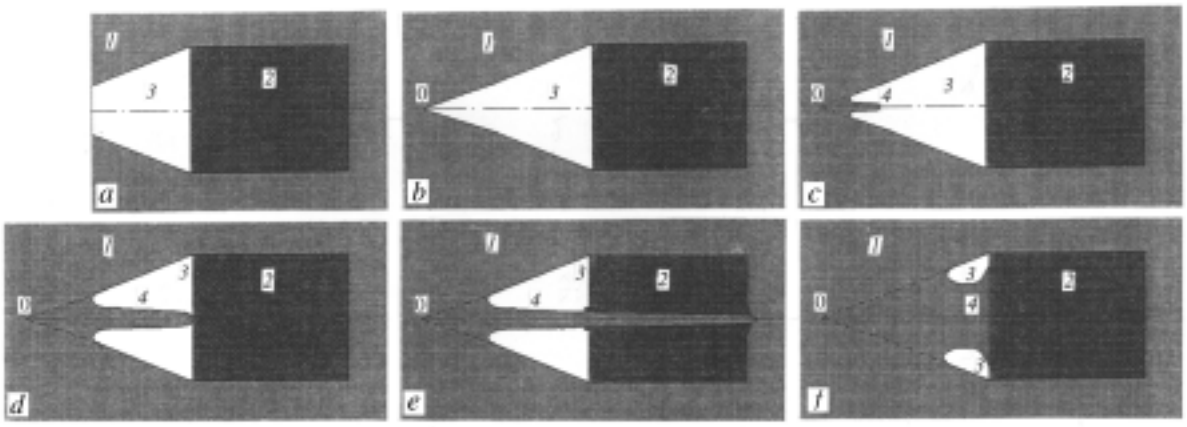

Fig. 7. Diagram of flow of a softened obstacle material around a particle: *a–f*) successive instants of time; 1) obstacle material; 2) particle; 3) channel; 4) cumulative jet.

energy in the form of a variable pressure field. The time of existence of such a pressure field corresponds to the complete period of loading of the obstacle by a gas-powder jet. According to the estimations made in [4, 8, 50, 51], such a repeated loading is capable of supplying the obstacle material with an energy sufficient for its partial (or locally total) disordering, which to a certain extent is confirmed by the numerical experiment [55]. However, the fact of disordering itself is insufficient to provide superdeep penetration. In [25], the estimations of the depth of penetration of individual microparticles into a steel melt are given. It is shown that the limiting depths attainable for particles moving with velocities which are characteristic of superdeep penetration do not exceed 100 gauges, whereas thousands or even tens of thousands of gauges are observed in practice. Consequently, the necessary condition of existence of superdeep penetration is the possibility of redistribution of the energy stored by the obstacle in the process of its treatment with a gas-powder flux in favor of a certain part of the particles of this flux. In this case, the mechanism of redistribution must provide for a single transfer of a certain, even if very large, part of the energy but its continuous delivery to the moving object. Otherwise, the penetration will decay rapidly, since spasmodically accelerated particles come to that region of interaction [17] where the influence of the thermal expenditure of energy increases markedly with a high probability of a local thermal explosion. Such a possible mechanism of energy redistribution has been proposed in [4, 8, 50, 51].

As has been noted above, "channels" formed by particles in an obstacle close (collapse) in the wake of moving strikers and can be found subsequently only as a result of the special procedure of pickling of metallographic sections which removes a strongly deformed obstacle material from the cavity of the "channel." The closing of the "channels" is determined by the existence of the pressure field generated by the gas-powder flux in the obstacle. Since in the evacuated space in the wake of the moving particle the pressure is much lower than in the obstacle, the "channel" begins to contract under the action of the arising difference between the forces (Fig. 7a). The dynamics of its contraction is shown in Fig. 7. After a time, the "channel" collapses at point 0 (Fig. 7b). When the angle of collapse is fairly large, at this point there arises a high-velocity jet (Fig. 7c) which very rapidly catches up with the particle (Fig. 7d). If the size of this particle is much larger than the diameter of the jet, the interaction regime where the jet "pierces" the particle becomes very probable (Fig. 7e). Otherwise, the high-velocity jet, retarding on the back surface of the moving striker (Fig. 7f), slightly pushes the particle, transferring a part of its energy to it. In this case, such an interaction regime can be established where the pushing compensates for the entire energy expended by the particle on penetration. The estimations made in [4, 8, 50, 51] give a sufficiently complete characteristic of this regime, and an exact interpretation of the equation of motion for a perfectly rigid axially symmetric particle under pushing conditions at variable and constant pressure fields is given in [44–46]. In this case, the particle moves in the obstacle with a velocity dependent mainly on the pressure generated in it by the particle flux. The time of motion is determined by the duration of the loading or by the time of existence of the striker (if it is shorter than the loading time.)

The considerations of Makarov [56], who proposed his version of the superdeep-penetration model are on the whole analogous to the considerations given in [44–46] and lead to a solution allowing the movement of a formation

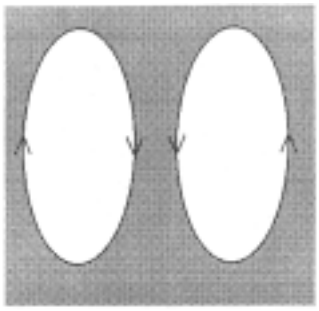

Fig. 8. Cumulative microvortex moving in the obstacle according to the assumption of Makarov [56].

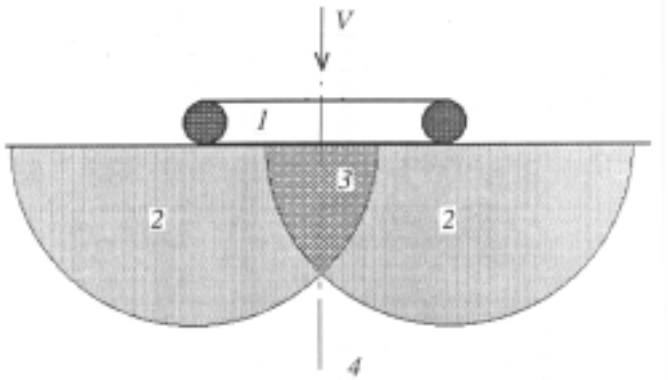

Fig. 9. Scheme of interaction of a ring object with an obstacle: 1) ring object; 2) material of the obstacle behind the front of primary waves from the ring object; 3) region of higher-than-average tensile stresses; 4) undisturbed material of the obstacle.

similar to the formation shown in Fig. 8 in the material of the obstacle. They can be used to estimate the parameters of motion of rapidly melting objects.

In any case, plastic models are characterized by a high degree of influence of the loading parameters (which is confirmed by experiment [8, 25]) on the results of superdeep penetration. The main disadvantage of these models is the lack of reliable, first of all experimental, information on the state of the obstacle in the period of loading, which prevents them from being conclusively and reliably substantiated. However, investigations of superdeep penetration have been developing very dynamically in recent times, which gives grounds to hope that the necessary data will be obtained.

3) *Shock-wave models.* One of the shock-wave models has been proposed in [57]. It assumes that some particles of the flux are entrained into the thickness of the obstacle by the shock wave generated by the flux ("on the wave crest" according to the terminology of [57]). In this case, the entrained objects can move to indefinitely large depths, because any energy loss will be compensated for with the shock wave. However, it should be noted that such an "entrainment" can occur only for objects whose dimensions are comparable to the thickness of the shock wave entraining them. In metals, this thickness is determined by the lattice parameter a and does not exceed $100a$ for the majority of them [58]. Since $a \le 10$ Å, the thickness of the shock-wave front in metals can be estimated at $\delta \le 10^{-10}$ m, which is deliberately smaller than the characteristic dimensions of the penetrating objects (10^{-6}–10^{-4} m). This means that for the shock-wave front a particle is a large macroformation the "entrainment" of which is unlikely.

Adadurov et al. [12] also present their vision of the problem of superdeep penetration. Investigating questions concerning the processes of wave formation on collision of ring-like objects with a solid obstacle, they have come to the conclusion that the specific interaction of shock waves occurs along the axis of symmetry (Fig. 9) (which was noted in due time by Barkhudarov et al. [59]), as a result of which the level of pressure in the region adjacent to the axis of symmetry exceeds markedly the pressure in the remaining material. The arising force is tensile in character. As a consequence, a specific region appears whose state and parameters can differ significantly from the initial ones.

Sometimes, the existence of such a region leads to the appearance of a macrocavity. Adadurov et al. [12, 60] assumed that the superdeep-penetration effect is due to the arrival of a particle at such a cavity. The appearance of the macrocavity itself is related to the "turning inside out" of the thin (1–1.5 mm) aluminum casing of the cumulative accelerator, which accelerates and rolls up into a ring under the action of the explosion wave. In their opinion, this ring collides flat with the obstacle surface, with the result that in it the required specific region of interaction is proposed (Fig. 9), into which the particles reaching the obstacle in the process of acceleration "fall." It should be noted that the "turning inside out" of the facing described in [12, 60] is sometimes observed in experiments [3], but this does not often occur. The fragments of the facing are usually strongly deformed, and they do not resemble a ring even approximately. Moreover, the variant that the facing falls flat on the obstacle surface is unlikely, because it is very difficult to provide the absolute symmetry of the scheme required for such an outcome. And the experiments carried out in [9–11] with the acceleration scheme free of a facing show that realization of the superdeep-penetration effect in accordance with the mechanism described in [12, 60] is absolutely improbable. Nonetheless, a series of experiments where the recess of the cumulative accelerator filled with a powder was free of a facing has been carried out [30]. The analysis of the results obtained has shown that superdeep penetration occurs in this case, too. Thus, the last-mentioned hypothesis has been checked experimentally. Negative results have been obtained.

In closing, it should be noted that the authors allow the probability of existence of any other models. But, as we know, they have not been discussed widely in the literature.

Prospects. At present, investigation of the process of superdeep penetration has come to a line where simple statement of the qualitative results ends and work on investigating its limits and essence and quantitative relations begins. Determination of the properties of materials subjected to treatment with a high-velocity gas-powder jet which results in superdeep penetration has become topical. Procedures for purposeful, quantitative-statistical study of the phenomenon have already been developed or are at the stage of active development. Problems concerning superdeep penetration are attracting the attention of an increasing number of scientists, which is explained by the extended range of the problems under study and the employed procedures and facilities. Moreover, healthy scientific competition will lead without fail to interesting scientific and technological results, which has repeatedly been proved in practice throughout the history of development of natural sciences.

The authors of this review realize that a number of works devoted to superdeep penetration are beyond their analysis for one reason or another. A certain number of the initial, pioneering investigations were intentionally omitted since their results became a constituent part of subsequent, more general works. Nonetheless, there is good reason to believe that the attempt at generalizing the results of investigations devoted to the problems of superdeep penetration will not be in vain and will stimulate further experimental and theoretical work in this field.

NOTATION

d, size of the penetrating particles (strikers), μm; *V*, velocity of the flux, m/sec; *a*, lattice parameter; δ, thickness of the shock-wave front; *c*, concentration, %; *L*, thickness of the front part, m.

REFERENCES

1. V. G. Gorobtsov, S. M. Usherenko, and V. Ya. Furs, *Poroshk. Metallurg.* (Minsk), Issue 3, 8–12 (1979).
2. K. I. Kozorezov, V. N. Maksimenko, and S. M. Usherenko, in: *Selected Problems of Modern Mechanics* [in Russian], Pt. 1, Moscow (1981), pp. 115–119.
3. S. M. Usherenko, *Conditions of Superdeep Penetration and Creation of the Process of Hardening of Tool Steels by a High-Speed Flux of Powder Materials*, Candidate's Dissertation (in Engineering), Minsk (1983).
4. S. K. Andilevko, G. S. Romanov, V. A. Shilkin, and S. M. Usherenko, *Int. J. Heat Mass Transfer*, **36**, No. 4, 1113–1124 (1993).
5. M. Jeandin, M. Vardavoulias, S. K. Andilevko, O. V. Roman, V. A. Shilkin, and S. M. Usherenko, *Revue de Metallurgie*, No. 12, 808–812 (1992).
6. S. S. Grigoryan, *Dokl. Akad. Nauk SSSR*, **292**, No. 6, 1319–1322 (1987).
7. G. G. Chernyi, *Dokl. Akad. Nauk SSSR*, **292**, No. 6, 1324–1328 (1987).

8. S. K. Andilevko, *Superdeep Mass Transfer of Discrete Microparticles in Metal Obstacles under Loading of the Latter by a Powder Flux*, Candidate's Dissertation (in Physics and Mathematics), Minsk (1991).
9. S. E. Aleksentseva, *Features of Dynamic Interaction of a Flux of High-Speed Powder Particles with Metals*, Candidate's Dissertation (in Physics and Mathematics), Samara (1997).
10. A. N. Bekrenev, R. G. Kirsanov, and A. L. Krivchenko, *Pis'ma Zh. Tekh. Fiz.*, **22**, Issue 2, 87–89 (1996).
11. R. G. Kirsanov, *Investigation of the Kinetics of Processes and of a Change in the Structure and Properties of Metals in the Case of the Shock-Wave Action of a Flux of Discrete Particles in the Mode of Superdeep Penetration*, Candidate's Dissertation (in Physics and Mathematics), Samara (1997).
12. G. A. Adadurov, A. F. Belikova, and S. N. Buravova, *Fiz. Goreniya Vzryva*, No. 4, 95–101 (1992).
13. V. A. Shilkin, *Structure and Properties of Heat-Treated R6M5 Steel Hardened by a High-Speed Flux of Powder Materials*, Candidate's Dissertation (in Engineering), Minsk (1986).
14. S. K. Andilevko, O. V. Roman, V. A. Shilkin, and S. M. Usherenko, *J. Physique IV*, **4**, No. 8, 795–801 (1994).
15. A. G. Bazilevskii and B. A. Ivanov, in: *Mechanics of Formation of Funnels on Impact and Explosion* [in Russian], Moscow (1977), pp. 172–227.
16. L. V. Leont'ev, A. V. Tarasov, and I. A. Tereshkin, *Kosmich. Issled.*, **9**, Issue 5, 796–798 (1971).
17. J. Zukas, in: *Shock Dynamics* [Russian translation], Moscow (1986), pp. 110–168.
18. E. I. Andriankin and Yu. S. Stepanov, *Kosmich. Issled.*, **6**, Issue 5, 752–797 (1968).
19. N. A. Zlatin, A. P. Krasil'nikov, G. I. Mishin, and N. N. Popov, *Ballistic Installations and Their Use in Experimental Investigations* [in Russian], Moscow (1974).
20. S. K. Andilevko, V. A. Shilkin, V. Slobodsky, and S. M. Usherenko, in: *Metallurgical and Material Application of Shock-Wave and High-Strain-Rate Phenomena*, USA (1995), pp. 361–368.
21. S. K. Andilevko, O. V. Roman, V. G. Gorobtsov, and S. M. Usherenko, *Poroshk. Metallurg.* (Minsk), No. 3, 100–102 (1987).
22. S. K. Andilevko, O. V. Roman, V. A. Shilkin, and S. M. Usherenko, *Khim. Fiz.*, **12**, No. 5, 34–41 (1993).
23. S. M. Usherenko, *Superdeep Penetration of Particles into Obstacles. Creation of Composite Materials* [in Russian], Minsk (1998).
24. S. K. Andilevko, O. A. Dybov, and O. V. Roman, *Inzh.-Fiz. Zh.*, **73**, No. 4, 797–801 (2000).
25. O. V. Roman, S. K. Andilevko, and S. S. Karpenko, *Scientific Research Report No. 19992123* [in Russian], Minsk (1999).
26. F. A. Baum, L. P. Orlenko, K. P. Stanyukovich, V. P. Chelyshev, and B. I. Shekhter, *Physics of Explosion* [in Russian], Moscow (1975).
27. S. K. Andilevko, O. V. Roman, V. A. Shilkin, and S. M. Usherenko, *J. Physique IV*, **4**, No. 8, 803–807 (1994).
28. S. K. Andilevko, O. V. Roman, O. A. Dybov, S. S. Karpenko, and O. I. Koval', *Dokl. Nats. Akad. Nauk Belarusi*, **44**, No. 5, 771–774 (2000).
29. O. V. Roman, S. K. Andilevko, S. S. Karpenko, and G. P. Okatova, *Inzh.-Fiz. Zh.*, **73**, No. 5, 1056–1063 (2000).
30. S. K. Andilevko, S. S. Karpenko, and V. A. Shilkin, *Pis'ma Zh. Tekh. Fiz.*, **25**, Issue 7, 69–73 (1999).
31. S. K. Andilevko, O. V. Roman, V. A. Shilkin, V. Slobodsky, and S. M. Usherenko, in: *Metallurgical and Material Application of Shock-Wave and High-Strain-Rate Phenomena*, USA (1995), pp. 437–443.
32. S. K. Andilevko, E. N. Sai, G. S. Romanov, and S. M. Usherenko, *Fiz. Goreniya Vzryva*, **24**, No. 5, 85–89 (1988).
33. S. M. Usherenko, V. F. Nozdrin, S. I. Gubenko, and G. S. Romanov, *Int. J. Heat Mass Transfer*, **37**, No. 15, 2367–2375 (1993).
34. S. M. Usherenko, S. I. Gubenko, and V. F. Nozdrin, *Metallofizika*, **13**, No. 7, 57–64 (1991).
35. S. K. Andilevko, E. A. Doroshkevich, V. A. Shilkin, and S. M. Usherenko, *Int. J. Heat Mass Transfer*, **41**, Nos. 6–7, 951–956 (1998).
36. S. K. Andilevko, G. S. Romanov, V. A. Shilkin, and S. M. Usherenko, *Pis'ma Zh. Tekh. Fiz.*, **16**, Issue 22, 42–44 (1990).

37. S. K. Andilevko, S. S. Karpenko, V. A. Shilkin, and O. A. Dybov, *Scientific Research Report No. 19992122* [in Russian], Minsk (1999).
38. S. K. Andilevko, V. A. Shilkin, and S. M. Usherenko, in: *Proc. Conf. "Shock Waves in Condensed Matter,"* St. Petersburg (1996), pp. 119–120.
39. I. G. Budkevich, O. A. Dybov, G. N. Dubrovskaya, and S. M. Usherenko, in: *Ext. Abstr. of Papers presented at All-Union Meeting "Use of High Pressures for Production of New Materials and Creation of Intense Processes of Chemical Technology"* [in Russian], Moscow (1986), p. 83.
40. G. N. Dubrovskaya, S. M. Usherenko, I. I. Borovinskaya, I. G. Budkevich, and O. A. Dybov, in: *Ext. Abstr. of Papers presented at the 1st All-Union Symp. on Macroscopic Kinetics and Chemical Gas Dynamics* [in Russian], Vol. 1, Alma-Ata (1984), p. 196.
41. S. K. Andilevko, O. V. Roman, G. S. Romanov, and S. M. Usherenko, *Poroshk. Metallurg.* (Minsk), Issue 9, 3–11 (1985).
42. S. K. Andilevko, V. G. Serov, V. A. Shilkin, and S. M. Usherenko, in: *High-Energy Treatment of Materials* [in Russian], Dnepropetrovsk (1997), pp. 8–14.
43. S. K. Andilevko, S. M. Usherenko, and V. A. Shikin, *Pis'ma Zh. Tekh. Fiz.*, **24**, No. 17, 67–69 (1998).
44. S. K. Andilevko, *Inzh.-Fiz. Zh.*, **71**, No. 3, 399–403 (1998).
45. S. K. Andilevko, *J. Physique IV*, **7**, 727–734 (1997).
46. S. K. Andilevko, *Int. J. Heat Mass Transfer*, **41**, Nos. 6–7, 957–962 (1998).
47. S. K. Andilevko, S. S. Karpenko, and O. V. Roman, *Inzh.-Fiz. Zh.*, **73**, No. 5, 1050–1055 (2000).
48. S. K. Andilevko, E. A. Doroshkevich, S. S. Karpenko, S. M. Usherenko, and V. A. Shilkin, *Inzh.-Fiz. Zh.*, **71**, No. 3, 394–398 (1998).
49. S. K. Andilevko, V. A. Shilkin, S. M. Usherenko, and I. G. Budkevich, *Scientific Research Report No. 19983283* [in Russian], Minsk (1998).
50. L. V. Al'tshuler, S. K. Andilevko, G. S. Romanov, and S. M. Usherenko, *Pis'ma Zh. Tekh. Fiz.*, **15**, Issue 5, 55–57 (1989).
51. L. V. Al'tshuler, S. K. Andilevko, G. S. Romanov, and S. M. Usherenko, *Inzh.-Fiz. Zh.*, **61**, No. 1, 41–45 (1991).
52. A. K. Kozorezov, K. I. Kozorezov, and L. I. Mirkin, *Fiz. Khim. Obrab. Mater.*, No. 2, 51–55 (1990).
53. K. I. Kozorezov and L. I. Mirkin, *Fiz. Khim. Obrab. Mater.*, No. 3, 75–79 (1999).
54. A. E. Rakhimov, *Vestn. MGU, Matematika Mekhanika, Ser. 1*, No. 5, 72–74 (1994).
55. A. I. Valishev and Yu. A. Trishin, in: *Mechanics of High-Speed Processes* [in Russian], Issue 51 (1981) pp. 30–41.
56. P. V. Makarov, in: *Chemical Physics of Combustion and Explosion Processes* [in Russian], Vol. 1, Pt. 2, Chernogolovka (1966), pp. 331–332.
57. V. A. Simonenko, N. A. Korkin, and V. V. Bashurov, *Problems of Nuclear Science and Technology. Theoretical and Applied Physics* [in Russian], Issue 1 (1988), pp. 85–91.
58. Ya. B. Zel'dovich and Yu. P. Raizer, *Physics of Shock Waves and High-Temeprature Hydrodynamic Phenomena* [in Russian], Moscow (1966).
59. E. M. Barkhudarov, M. O. Mdivanishvili, V. I. Sokolov, N. I. Taktakishvili, and V. E. Terekhin, *Izv. Akad. Nauk SSSR, Mekh. Zhidk. Gaza*, No. 5, 107–111 (1990).
60. R. D. Yound, D. L. Littlefield, and V. Horic, in: *Proc. AIP Conf.*, USA, Vol. 309, No. 1, 1821–1824 (1994).